Strain-Driven and Ultrasensitive Resistive Sensor/Switch Based on Conductive Alginate/Nitrogen-Doped Carbon-Nanotube-Supported Ag Hybrid Aerogels with Pyramid Design

Songfang Zhao,[†,‡] Guoping Zhang,*[,†,§] Yongju Gao,[†] Libo Deng,[†] Jinhui Li,[†,‡] Rong Sun,*[,†] and Ching-Ping Wong[§,∥]

[†]Shenzhen Institutes of Advanced Technology, University of Chinese Academy of Sciences, Shenzhen 518055, China

[‡]Shenzhen College of Advanced Technology, University of Chinese Academy of Sciences, Shenzhen 518055, China

[§]School of Materials Science and Engineering, Georgia Institute of Technology, 771 Ferst Drive, Atlanta, Georgia 30332, United States

[∥]Department of Electronic Engineering, Faculty of Engineering, The Chinese University of Hong Kong, Hong Kong, China

Ⓢ Supporting Information

ABSTRACT: Flexible strain-driven sensor is an essential component in the flexible electronics. Especially, high durability and sensitivity to strain are required. Here, we present an efficient and low-cost fabrication strategy to construct a highly sensitive and flexible pressure sensor based on a conductive, elastic aerogel with pyramid design. When pressure is loaded, the contact area between the interfaces of the conductive aerogel and the copper electrode as well as among the building blocks of the nitrogen-doped carbon-nanotube-supported Ag (N-CNTs/Ag) aerogel monoliths, changes in reversible and directional manners. This contact resistance mechanism enables the hybrid aerogels to act as strain-driven sensors with high sensitivity and excellent on/off swithcing behavior, and the gauge factor (GF) is ∼15 under strain of 3%, which is superior to those reported for other aerogels. In addition, robust, elastomeric and conductive nanocomposites can be fabricated by injecting polydimethylsiloxane (PDMS) into alginate/N-CNTs/Ag aerogels. Importantly, the building blocks forming the aerogels retain their initial contact and percolation after undergoing large-strain deformation, PDMS infiltration, and cross-linking of PDMS, suggesting their potential applications as strain sensors.

Dimension of top electrode on GF

KEYWORDS: strain-driven, pyramid design, contact resistance, conductive hybrid aerogel, flexible
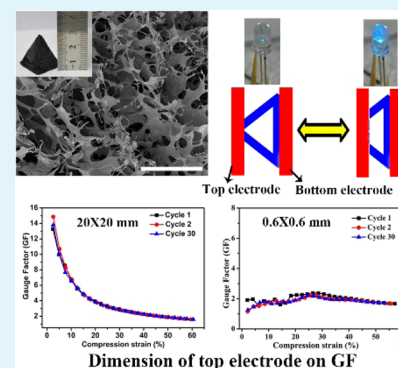
1. INTRODUCTION

Strain regulation of flexible and ultrasensitive sensors/switches has attracted extensive attention in the fields of nano- or microelectromechanical systems (N/MEMS) and wearable health monitors. Especially, these applications require sensors/switches with high sensitivity to reflect the location of strain imposed via the variation of resistance or to record a human pulse wave while facilitating conformal attachment to a soft, curved surface (e.g., human skin).[1−6] Conventionally, to measure the spatial distribution of an input pressure signal effectively, a number of circuit elements involving elastic microstructured conducting polymers,[2,7] hybrid composites,[8,9] and nanowire or nanotube assemblies[10−12] were needed to be integrated on various flexible substrates. A striking example of a flexible and highly sensitive strain-gauge sensor has been demonstrated recently by Suh, in which numerous metal-coated, high-aspect-ratio nanofibers were monolithically assembled on polydimethylsilixane (PDMS) surfaces.[13] Despite the potential and high performance of these devices, a highly sensitive sensor capable of working at high strains remains a great challenge. It is because these flexible sensors with

nanomaterial assemblies need special nanostructure design, and thus their manufacture is complicated and expensive.

Piezoresistive sensors/switches, which transduce a mechanical strain into an impedance change, have been widely used owing to their attractive advantages, including their simple read-out mechanism, sensitivity to both strain and flexion, and feasible preparation. In this case, the change in conductance or resistance can be measured from a specific active matrix with or without an on/off switchable transistor.[14−16] Among them, the current mainstream strategy in attempting to achieve high sensitivity is to engineer new structural constructs from established materials.[14,17−20] For example, the pressure sensors based on fractured graphene-wrapped polyurethane sponge have been designed for artificial electronic skin application, which possess high sensitivity, long cycling life, and could be readily scaled up.[14] Alternatively, a related sensing mechanism involves utilizing the contact resistance between the interfaces
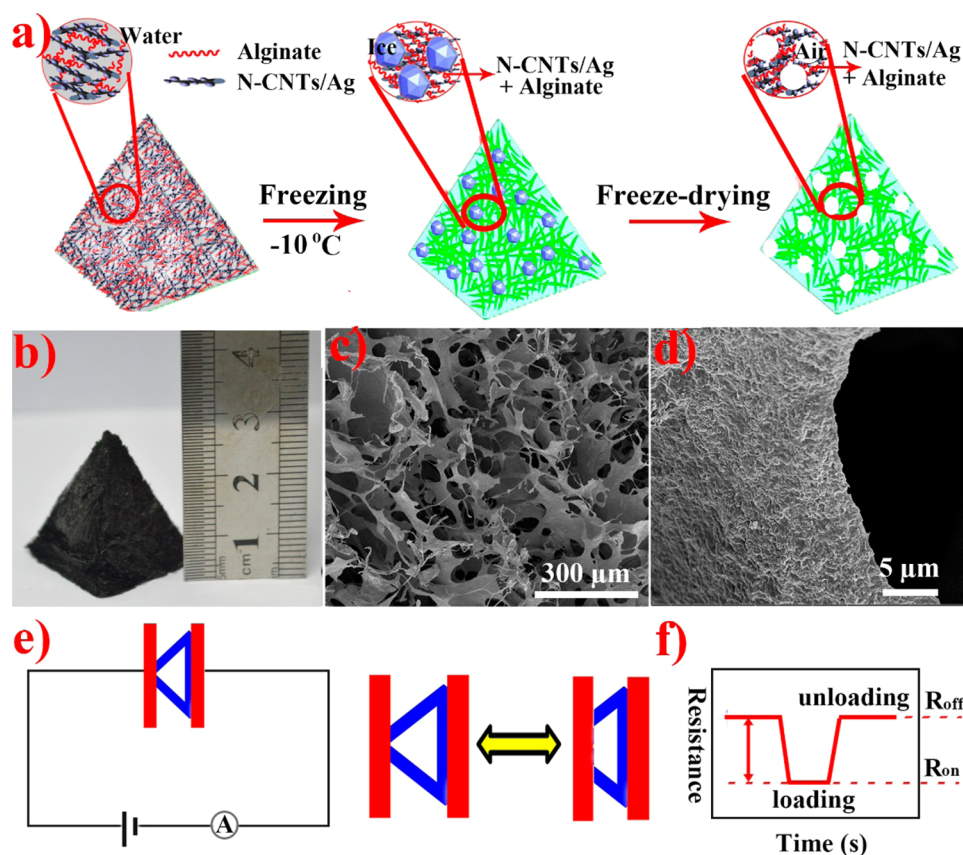
Figure 1. Flexible and strain-driven sensor/switch based on pyramid design. (a) Schematic illustration of the fabrication of a flexible hybrid aerogel. (b) Photographic image. (c, d) SEM images of cross-section of hybrid aerogel at different magnifications. (e) Schematic illustration of the sensing mechanism. (f) Electrical resistance changes in response to loading and unloading (R_{off} = unloading, R_{on} = loading).

of the electrodes and conductive sponges, which could offer high sensitivity and a large working range.[12,16]

Herein, inspired by the above mechanism, first, we have developed flexible and ultrasensitive aerogels by combining alginate and nitrogen-doped carbon-nanotube-supported Ag (N-CNTs/Ag) in a synergistic manner. In more details, an alginate chain comprises mannuronic acid (M unit) and guluronic acid (G unit), arranged in blocks rich in G units, blocks rich in M units, and blocks of alternating G and M units (Supporting Information Figure S2). Their excellent mechanical properties and biological compatibility, as available from widely abundant sustainable seaweed and facile processes could be further functionalized by N-CNTs/Ag, thus combining the biological compatibility and superior electrical properties of N-CNTs/Ag.[21,22] Then we introduce a novel strain-gauge sensor with structural design, in which the active component with pyramid shape is both conductive and elastic. The key novelty of our sensor is to tune hierarchical structure which includes nanostructure (design of N-CNTs/Ag hybrids), microstructure (design of conductive aerogel) and macro-structure (design of pyramid shape) to achieve a superior strain-gauge sensor. Typically, a sensitivity of ~15 of gauge factor has been achieved due to contact resistance mechanism, which is higher than those reported recently.[12,13,23] Furthermore, negligible loading−unloading signal changes are observed over multiple cycles. Notably, the key sensing elements and sensor package could be easily fabricated in large scale at low-cost. These novel structure and package design will enable their potential applications in detecting various extern stimulus.

2. MATERIALS AND METHODS

2.1. Synthesis of N-CNTs/Ag Hybrids. The water-dispersible N-CNTs/Ag hybrids are synthesized according to our previous work.[22] Typically, 25 mg of N-CNTs-COOH is mixed with 5 mL of DMSO solution containing dicyclohexylcarbodiimide (DCC, 20 mg) and 4-(dimethylamino) pyridine (DMAP, 15 mg). The 3 mL DMSO solution of hyperbranched polyglycerol (HPG) (75 mg) is then added into the above mixture at 50 °C under magnetic stirring for 24 h. AgNO$_3$ /DMSO (15 mg/2 mL) solution is introduced into the above mixture under magnetic stirring for 2 h, and then the L-ascorbic acid (LAA)/DMSO (9 mg/2 mL) solution is poured into the above mixture and stirs at room temperature for another 3h. The resultant solid product (N-CNTs/Ag) is collected by filtration.

2.2. Fabrication of Alginate/N-CNTs/Ag Hybrid Aerogels by Ice-Template. Alginate/N-CNTs/Ag aerogels are fabricated according to the previously reported ice-template process.[24] Briefly, an aqueous solution of N-CNTs/Ag (20 mg/mL) with different amount of alginate solution is frozen by pouring them into the designed molds followed by freeze-drying for 2 days.

2.3. Characterization. The morphology and microstructure are investigated by field-emission scanning electron microscopy (FE-SEM, nanoSEM 450, NOVA, USA). Before observation, the samples are coated with gold. The rheological behavior is measured using an Anton Paar MCR 302 rheometer. The electrical resistance variation is recorded by a two-probe method under different mechanical deformation. In the measurement, two copper sheets serve as electrodes to connect to aerogels and a Keithly 2410 Source Meter instrument. Every electromechanical experiment is repeated by 3 times and the value of electrical-resistance is the average value. The compression stress−strain measurements are performed by using an electronic universal testing machine (RGM-4000, REGER Co. Ltd., China) with two test plates. The samples are set on the lower plate
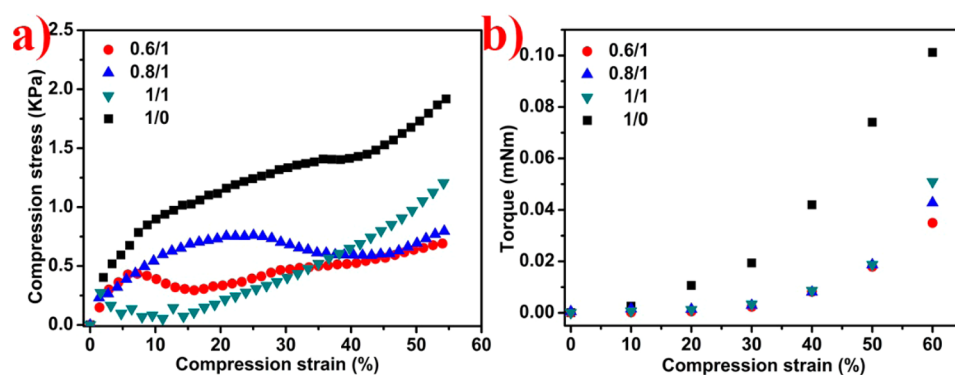
Figure 2. (a) Compression stress−strain curves of alginate/N-CNTs/Ag hybrid aerogels and (b) rheological torque-strain curves of alginate/N-CNTs/Ag hybrid aerogels at 10 rad s^{-1}. Note that the ratio in label is the ratio of total weight of alginate to the total weight of N-CNTs/Ag hybrids.
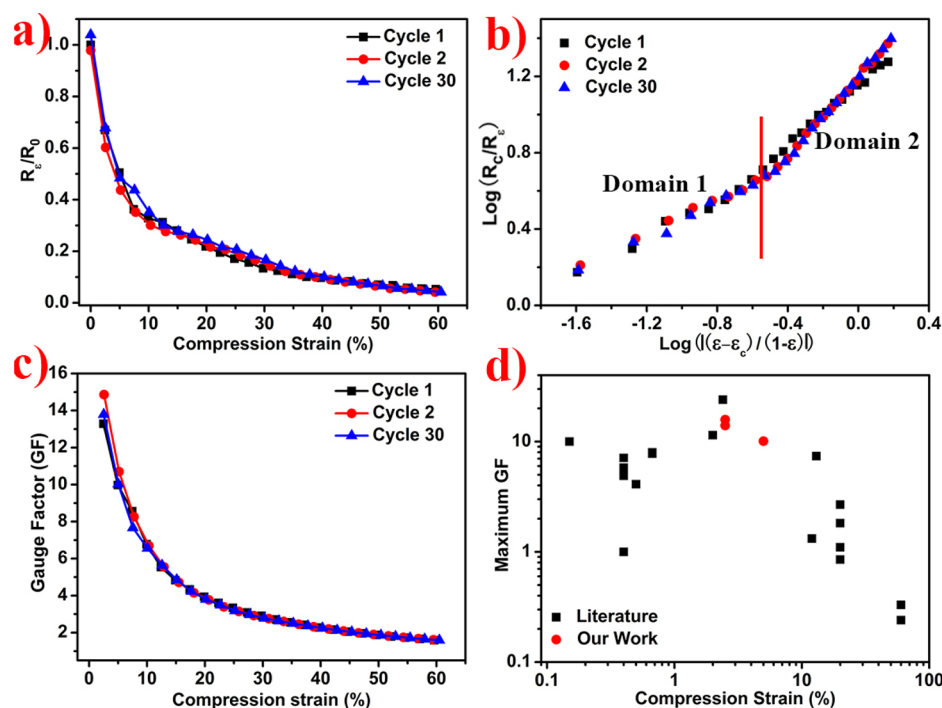

Figure 3. Electrical properties of composite aerogel (0.8:1) under compression strain. (a) Plots of electrical resistance as a function of compression strain after repeated loading−unloading cycles. (b) Plots of R_c/R_ε versus $|(\varepsilon - \varepsilon_c)/(1 - \varepsilon)|$ (log−log scale). Note that $1/R_\varepsilon$ is proportional to σ_ε and $1/R_c$ is proportional to σ_c. (c) Gauge factor (GF) plotted versus compression strain. (d) Summary of results from literatures about strain sensors (pressure stimulus). The maximum reported values of GF plotted versus the corresponding compression strain. Also plotted are the results obtained in our work.

and compressed by the upper plate connecting to a load cell. The strain ramp rate is controlled to be 1 mm min^{-1} for the measurements.

3. RESULTS AND DISCUSSION

3.1. Hybrid Aerogel Fabrication and Structure Characterization. Figure 1a illustrates the fabrication process of alginate/N-CNTs/Ag hybrid aerogels with pyramid shape. Briefly, N-CNTs/Ag hybrids are synthesized following our previous work.[22] Note that the interconnection among N-CNTs/Ag hybrids is constructed utilizing HPG as bridges via esterification and silver nanoparticles (NPs) are decorated on N-CNTs using HPG as templates. Next, the N-CNTs/Ag hybrids are purified by filtration and redispersed in alginate aqueous solution, which is poured into pyramid mold and followed by a freeze-drying process to prepare highly porous alginate/N-CNTs/Ag hybrid aerogel. Figure 1b shows the photographic image of a typical pyramid hybrid aerogel that has

a density of c.a. Twenty mg mL^{-1}. Further characterizations by SEM (Figure 1c and d, Supporting Information Figure S3) demonstrate sheet-like structure of micrometers lateral dimensions, as connected by nanofiber or nanotube bundles. The sheet-like aggregation could be explained by that plastic mold slows down the thermal transfer between the samples and outer condition (−10 °C) upon immersing the room-temperature suspension in this relative low temperature. Therefore, the ice crystals have enough time to grow larger, leading to the coaggregation of nanotubes and nanofibrils into hybrid sheets because of the direct affinity between benzene rings of CNTs and alginate, and the hydrogen bonds between the N-CNTs/Ag and alginate.[25]

The sensing mechanism includes strain-dependent contact resistance between the interfaces of the hybrid aerogel and copper electrodes, and strain-dependent contact resistace

22825

dx.doi.org/10.1021/am5069936 | ACS Appl. Mater. Interfaces 2014, 6, 22823−22829

among N-CNTs/Ag in hybrid aerogel monolith. Unlike a regular bulk rigid metal, pyramid sensor has porous structure and variable top electrode areas. The total contact areas among N-CNTs/Ag, aerogel and copper electrodes depend on the external strain applied. While applying an external pressure, a small compression deformation of aerogel enables more N-CNTs/Ag to contact with N-CNTs/Ag and copper electrodes, resulting more conductive pathways to convert into a change in the electrical resistance signal (Figure 1e and f). Upon unloading, the aerogel recoveres to its original shape, reducing the conductive pathways.

3.2. Mechanical and Rheological Properties. The stress−strain curves under compression deformation are shown in Figure 2a. The loading process of alginate aerogel exhibits three distinct deformation stages: a linear-elastic region for $\varepsilon < 10\%$, a plateau region for $10 < \varepsilon < 40\%$, and a steep slope region for $\varepsilon > 40\%$. Moreover, the essentially linear stress−strain curve at low strain without yield point indicates a ductile behavior of alginate aerogel with reduced brittleness, as expected for cellulose.[25] Upon combining N-CNTs/Ag with alginate, the shape of the stress−strain curves remain qualitatively similar, but the maximum stress decreases, which is because of plasticization of N-CNTs/Ag to the composites, the flexible bridges among N-CNTs/Ag, and the fewer number of interaction sites in the N-CNTs/Ag hybrids when compared with the large mumber of polar groups in alginate.

To further investigate the dynamic stability of alginate/N-CNTs/Ag hybrid aerogels, the rheological behaviors are investigated (Figure 2b and Supporting Information Figure S4). Small-deformation oscillatory measurements reveal that the torque is nearly independent of the frequency (ω) from 1 to 100 rad s^{-1} and the value of torque increases with strain, which is attributed to the increase of contact area during oscillatory test and dense cross-linking nodes. When it is compressed to a certain strain, the increasing contact area and denser nodes can offer more restorative force to resist the exercised torque.[26] Furthermore, the introduction of N-CNTs/Ag could also decrease the torque, which is attributed to the plasticization of fillers.[27]

3.3. Cyclic Tests and Sensitivity. To depict outputs from mechanical stimulus, we record changes in the electrical resistance as a function of applied strain for pressure (Figure 3 and Supporting Information Figure S5). It can be seen that the electrical resistance decreases sharply at the initial stage of compression and then decreases gradually beyond a strain of ∼25%. The turning points are consistent with those obtained from the curves in Supporting Information Figure S1c, which originate from pressure-driven percolation conductivity and electrode area changes.[28,29]

The electrical properties of composite aerogel composed of conductive fillers and insulating matrix are generally described by the percolation theory. The pressure-controlled percolation conductivity in terms of strain can be written as a power law function:[28,30]

$$\sigma(\varepsilon)_{\varepsilon > \varepsilon_c} \infty \sigma_c \left| \frac{\varepsilon - \varepsilon_c}{1 - \varepsilon} \right|^{\mu}$$

Where $\sigma(\varepsilon)$ is the conductivity at the strain ε, σ_c is the conductivity percolation threshold at the strain ε_c, and μ is the conductivity exponent. Now we assume that our alginate/N-CNTs/Ag aerogel monolith obeys the above theory and $\varepsilon_c = 0$ since all our N-CNTs/Ag aerogels are conductive without strain. To better understand this, we plot the R_c/R_ε versus $|(\varepsilon - \varepsilon_c)/(1 - \varepsilon)|$ in logarithmic scale in Figure 3b, which manifests two evident domains (divided by turning points) with different exponents of the power law, that is 0.45 and 0.82. This behavior is reproducible and repeatable in multiple cycles. The excellent linear relationships in respective domain validate the percolation theory. However, the values of the exponents are much less than the universal value of $\mu = 2.0$ expected for 3D systems.[28] The apparent discrepancy in conductivity exponents could be explained since our systems are far beyond the conductivity percolation threshold. Interestingly, obvious sharp transitions in Figure 3a and b demonstrate the presence of another "conductivity threshold". This may be attributed to the percolation of porous structures under compression strain: the conductivity in domain 1 may be due to the deformation of pores accompanying squeezing air out the matrix and increase of contact electrode areas; the conductivity in domain 2 may be due to the densification of N-CNTs/Ag and increase of contact electrode areas.

To assess the ability of our aerogel as a strain-gauge sensor, the GF is measured, which is usually defined as the relative change in electrical resistance ($\Delta R/R_0$) to the mechanical strain (ε).[31] For our case, the forces are applied in normal direction, causing the changes of the height and contact electrode areas. The measured values of GF are plotted as a function of applied strain in Figure 3c. Notably, we obtain a GF of 14 at a strain of ∼3%, which is approximately ten times more than our previous values obtained from cylinder aerogels.[22] This means that contact resistance mechanism plays an important role in resistance changes. Interestingly, the resistance changes become more sensitive to strain when less N-CNTs/Ag hybrids are introduced (Supporting Information Figure S5). In the aerogel with less N-CNTs/Ag, the connection among the N-CNTs/Ag is not fully established, and the external loading would increase the number of connection nodes, which substantially increases the percolation conductivity. Whereas, percolation conducting networks have been established among denser N-CNTs/Ag building blocks. Therefore, the compression strain would not affect the connection network of N-CNTs/Ag significantly, leading to only slight resistance variation.

The maximum observed gauge factor for pressure (∼15) is relatively high compared to values reported in literature (Supporting Information Table S1). To compare these values, we plot a map of the maximum values of both GF and the corresponding operating strain for a range of nanocomposite strain sensors from both the literatures and the study described here (Figure 3d and Supporting Information Table S1). It could be seen that we have achieved comparable gauge factor from our novel structural design.

The unique properties of strain-driven resistance changes enable our alginate/N-CNTs/Ag composite aerogels to directly act as elastomeric resistor switches. To depict piezoresistive effects visually, an alginate/N-CNTs/Ag composite aerogel is connected to light-emitting diode (LED) and power source in series. As shown in Supporting Information Movie S1, LED lamp exhibits enhanced bright light while loading the strain and then the lamp becomes darker while releasing the strain. Under compression strain, the resistance of the aerogel decreases, thus more partial voltage is dispensed to the LED lamp to make it brighter; while releasing, the elastic aerogel returns to its original state and recovers its large resistance, dispensing less partial voltage to the LED lamp to make it dark.

3.4. Contact Resistance Mechanism of Hybrid Aerogels Piezoresistance. As we know, the pressure sensors

22826

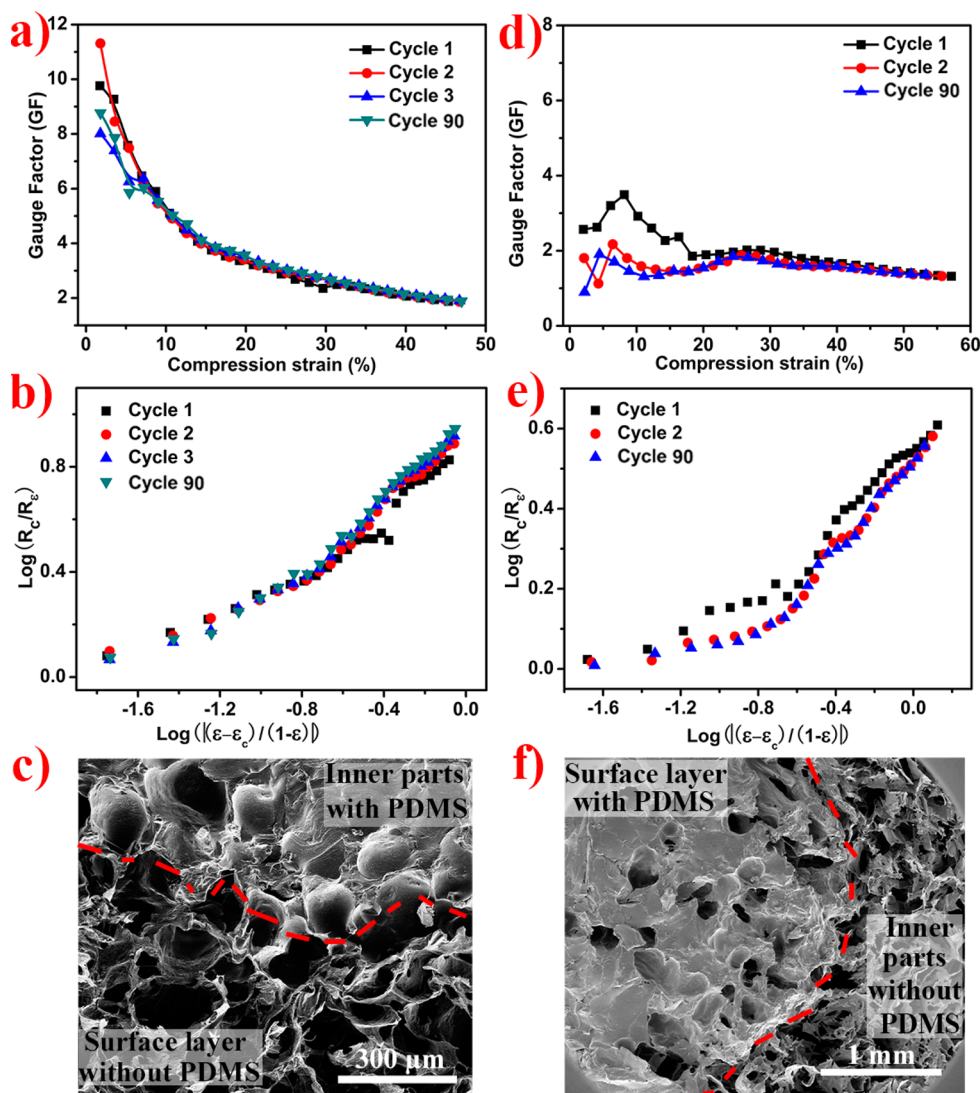dx.doi.org/10.1021/am5069936 | *ACS Appl. Mater. Interfaces* 2014, 6, 22823−22829

Figure 4. Comparison between different package manners in Supporting Information Figure S7b and d on electrical properties and microstructure. (a, d) Plots of GF as a function of compression strain after repeated loading–unloading cycles. (b, e) Plots of R_c/R_ε versus $|(\varepsilon - \varepsilon_c)/(1 - \varepsilon)|$(log–log scale). Note that $1/R_\varepsilon$ is proportional to σ_ε and $1/R_c$ is proportional to σ_c. (c, f) SEM image of cross section of alginate/N-CNTs/Ag aerogel-PDMS nanocomposite, (c) the surface has little PDMS infiltrated, indicating that this injection package could realize the contact resistance mechanism between the interfaces of the copper electrode and conductive aerogel, (f) the surface has more PDMS coated, indicating that this surface coating package could prevent the occurrence of contact resistance changes between the interfaces of the copper electrode and conductive aerogel.

operate primarily through a contact resistance mechanism, that is, the piezoresistance is realized via the variations of physical contact area of the whole sensors. Simultaneously, an important question arises as to whether the contact resistance between the interfaces of the copper electrode and a conductive aerogel or contact resistance among N-CNTs/Ag building blocks of aerogel is dominantly responsible for the high sensitivity. To address this, we utilize a sandwich geometry with deliberately designed top electrode to eliminate the variations of contact area between the interfaces of the conductive aerogel and the copper electrode (Supporting Information Figure S6). It can be seen that the GF decrease dramatically to ~2, indicating the piezoresistance can be attributed to the contact resistance between the interfaces of the conductive aerogel and the electrode, which is consistent with previous researches.[12,16]

To enhance the robustness of the aerogel, two kinds of alginate/N-CNTs/Ag/PDMS conductive composites are prepared. First, we directly inject PDMS/CHCl$_3$ solution into

alginate/N-CNTs/Ag hybrid aerogel to prepare electrically conductive nanocomposites (Supporting Information Figure S7b). The process involves the injection of dilute PDMS solution and subsequent infiltration into the pores by capillarity, and then the curing of resultant composites at 40 °C for 24 h. Note that diluted PDMS may permeate to surface layer of aerogel due to its low viscosity and the composites shrink slightly due to the evaporation of CHCl$_3$. When the aerogel is filled with PDMS, its maximum compressive load is enhanced by 6-fold, that is, up to ~1.2 N (Supporting Information Figure S8b). However, the change of electric resistance is negligible, which indicates that the percolated three-dimensional networks are still maintained and the curing of PDMS molecular does not destroy the contact among the N-CNTs/Ag. The electric resistance of nanocomposites also varies with compression deformation and the GF decreased by 10% at the initial deformation stage (Figure 4a and b). These phenomenons could be explained from the following aspects:

first, a small amount of diluted PDMS solution infiltrates the surface layer of aerogel and then is cured into the insulating layer, which inhibits the increase of contact areas between the interfaces of copper electrode and conductive composites (Figure 4c and Supporting Information Figure S8). Moreover, the presence of PDMS layer in pores inhibits the increase of interface contact spots among N-CNTs/Ag building blocks. With further compression deformation, the increase of contact areas between the interfaces of the conductive composites and the electrode and interface contact spots among N-CNTs/Ag become smoothly, leading to low sensitivity at higher strain.[32] This observation is consistent with the results as shown in Supporting Information Figure S1c.

Simultaneouly, we coat the surface layer of the aerogel using PDMS (Figure 4f and Supporting Information Figure S7c), which not only enhances its robustness but also prevents the occurrence of contact area changes between the interfaces of the electrode and conductive aerogel. Compared with results of Figure 3c, the GF decreases significantly at the initial deformation stage and the GF is maintained at a relatively constant value (below 2) after 90 cyclic tests (Figure 4d and e), implying the pressure sensitivity could be tuned by controlling the contact resistance between the interfaces of the copper electrode and a conductive aerogel. These observations are also consistent with our calculated results in Supporting Information Figure S1, that aerogels with pyramid shape have higher sensitivity to strain.

Furthermore, to assess the mechanical properties of these devices packaged with different manners (Supporting Information Figure S7), we measure the applied force versus strain (Supporting Information Figure S9). Only the first cycle of compression induced a slight plastic deforamtion, and the subsequent cycles are reversible. Note that output drift induced from the first several compression in porous polymers, and the as-prepared aerogels are subjected to a force loaded to eliminate the compression-induced plastic effect. Hysteresis loop formed by the loading and unloading curves is quantified as the main difference in energy dissipation during compression.[33,34] The energy dissipation is mostly caused by the friction between building blocks or movement of air through the pores. From the area of hysteresis loop divided by the full-scale output, it could be seen that aerogel packaged with PDMS or spacer could reduce the energy dissipation and plastic deformation in compression. It is worth noting that the package should guarantee the occurrence of the contact resistance mechanism between the interfaces of the conductive aerogel and electrode to achieve high sensitivity. The outstanding mechanical robustness and electrical conductivity in conjunction with high sensitivity enable its application as elastic sensors (Supporting Information Movie S2).

4. CONCLUSION

In summary, we have demonstrated a cost-effective approach for producing alginate/N-CNTs/Ag hybrid aerogel with pyramid shape, endowing the aerogel with high flexibility and sensitivity to strain by tuning its hierarchical structure. The experimental results show that the GF is ~15 at a strain of 3%, which is fairly comparable or superior to those of reported aerogels under pressure. The piezoresistance mainly originates from the contact resistance between the interfaces of conductive aerogel and electrode, which is confirmed by electrode design and packaging manners, respectively. Moreover, the robust, elastomeric and conductive nanocomposites

are fabricated by filling the PDMS into alginate/N-CNTs/Ag aerogels, and the GF is reproducible and kept at ~9 after 90 cycles because of their percolation maintained during large-strain deformation, polymer infiltration, and cross-linking process. We believe that our novel methodology represents a new low-cost approach to highly sensitive pressure sensor with a broad spectrum of applications such as in flexible touch displays and prosthetic skins.

■ ASSOCIATED CONTENT

ⓢ Supporting Information

Comparison of sensitivity of resistive pressure sensors and movies showing resistance under compression strain and sensitivity. This material is available free of charge via the Internet at http://pubs.acs.org.

■ AUTHOR INFORMATION

Corresponding Authors
*E-mail: gp.zhang@siat.ac.cn.
*E-mail: rong.sun@siat.ac.cn.
Notes
The authors declare no competing financial interest.

■ ACKNOWLEDGMENTS

■ REFERENCES

(1) Shin, U. H.; Jeong, D. W.; Park, S. M.; Kim, S. H.; Lee, W. H.; Kim, J. M. Highly Stretchable Conductors and Piezocapacitive Strain Gauges Based on Simple Contact-Transfer Patterning of Carbon Nanotube Forests. *Carbon* **2014**, *80*, 396−404.

(2) Choong, C. L.; Shim, M. B.; Lee, B. S.; Jeon, S.; Ko, D. S.; Kang, T. H.; Bae, J.; Lee, S. H.; Byun, K. E.; Im, J.; Jeong, Y. J.; Park, C. E.; Park, J. J.; Chung, U. Highly Stretchable Resistive Pressure Sensors Using a Conductive Elastomeric Composite on a Micropyramid Array. *Adv. Mater.* **2014**, *26*, 3451−3458.

(3) Segev-Bar, M.; Haick, H. Flexible Sensors Based on Nanoparticles. *ACS Nano* **2013**, *7*, 8366−8378.

(4) Liao, M. Y.; Hishita, S.; Watanabe, E.; Koizumi, S.; Koide, Y. Suspended Single-Crystal Diamond Nanowires for High-Performance Nanoelectromechanical Switches. *Adv. Mater.* **2010**, *22*, 5393−5397.

(5) Lu, N. S.; Lu, C.; Yang, S. X.; Rogers, J. Highly Sensitive Skin-Mountable Strain Gauges Based Entirely on Elastomers. *Adv. Funct. Mater.* **2012**, *22*, 4044−4050.

(6) Harris, J. M.; Lyer, G. R. S.; Bernhardt, A. K.; Huh, Y. J.; Hudson, S. D.; Fagan, J. A.; Hobbie, E. K. Electronic Durability of Flexible Transparent Films from Type-Specific Single-Wall Carbon Nanotubes. *ACS Nano* **2012**, *6*, 881−887.

(7) Park, J.; Lee, Y.; Hong, J.; Ha, M.; Jung, Y. D.; Lim, H.; Kim, S. Y.; Ko, H. Giant Tunneling Piezoresistance of Composite Elastomers with Interlocked Microdome Arrays for Ultrasensitive and Multimodal Electronic Skins. *ACS Nano* **2014**, *8*, 4689−4697.

(8) Radha, B.; Sagade, A. A.; Kulkarni, G. U. Flexible and Semitransparent Strain Sensors Based on Micromolded Pd Nanoparticle−Carbon μ-Stripes. *ACS Appl. Mater. Interfaces* **2011**, *3*, 2173−2178.

(9) Dvir, T.; Timko, B. P.; Brigham, M. D.; Naik, S. R.; Karajanagi, S. S.; Levy, O.; Jin, H. W.; Parker, K. K.; Langer, R.; Kohane, D. S. Nanowired Three-Dimensional Cardiac Patches. *Nat. Nanotechnol.* **2011**, *6*, 720−725.

(10) Takei, K.; Takahashi, T.; Ho, J. C.; Ko, H.; Gillies, A. G.; Leu, P. W.; Fearing, R. S.; Javey, A. Nanowire Active Matrix Circuitry for Low-Voltage Macro-Scale Artificial Skin. *Nat. Mater.* **2010**, *9*, 821−826.

(11) Amjadi, M.; Pichitpajongkit, A.; Lee, S. J.; Ryu, S.; Park, I. Highly Stretchable and Sensitive Strain Sensor Based on Silver Nanowire−Elastomer Nanocomposite. *ACS Nano* **2014**, *8*, 5154−5163.

(12) Gong, S.; Schawalb, W.; Wang, Y. W.; Chen, Y.; Tang, Y.; Si, J.; Shirinzadeh, B.; Cheng, W. L. A Wearable and Highly Sensitive Pressure Sensor with Ultrathin Gold Nanowires. *Nat. Commun.* **2013**, DOI: 10.1038/ncomms4132.

(13) Pang, C.; Lee, G. Y.; Kim, T.; Kim, S. M.; Kim, H. N.; Ahn, S. H.; Suh, K. Y. A Flexible and Highly Sensitive Strain-Gauge Sensor using Reversible Interlocking of Nanofibres. *Nat. Mater.* **2012**, *11*, 795−801.

(14) Yao, H. B.; Ge, J.; Wang, C. F.; Wang, X.; Hu, W.; Zheng, Z. J.; Ni, Y.; Yu, S. H. A Flexible and Highly Pressure-Sensitive Graphene-Polyurethane Sponge Based on Fractured Microstructure Design. *Adv. Mater.* **2013**, *25*, 6692−6698.

(15) Maheshwari, V.; Saraf, R. Tactile Devices To Sense Touch on a Par with a Human Finger. *Angew. Chem., Int. Ed.* **2008**, *47*, 7808−7826.

(16) Pan, L. J.; Chortos, A.; Yu, G. H.; Wang, Y. Q.; Isaacson, S.; Allen, R.; Shi, Y.; Dauskardt, R.; Bao, Z. N. An Ultra-Sensitive Resistive Pressure Sensor Based on Hollow-Sphere Microstructure Induced Elasticity in Conducting Polymer Film. *Nat. Commun.* **2014**, DOI: 10.1036/ncomms4002.

(17) Yamada, T.; Hayamizu, Y.; Yamamoto, Y.; Yomogida, Y.; Izadi-Najafabadi, A.; Futaba, D. N.; Hata, K. A Stretchable Carbon Nanotube Strain Sensor for Human-motion Detection. *Nat. Nanotechnol.* **2011**, *6*, 296−301.

(18) Khang, D. Y.; Jiang, H.; Huang, Y.; Rogers, J. A. A Stretchable Form of Single-Crystal Silicon for High-Performance Electronics on Rubber Substrates. *Science* **2006**, *311*, 208−212.

(19) Kim, D. H.; Ahn, J. H.; Choi, W. M.; Kim, H. S.; Kim, T. H.; Song, J. Z.; Huang, Y. G. Y.; Liu, Z. J.; Lu, C.; Rogers, J. A. Stretchable and Foldable Silicon Integrated Circuits. *Science* **2008**, *320*, 507−511.

(20) Park, M.; Im, J.; Shin, M.; Min, Y.; Park, J.; Cho, H.; Park, S.; Shim, M. B.; Jeon, S.; Chung, D. Y.; Bae, J.; Park, J.; Jeong, U.; Kim, K. Highly Stretchable Electric Circuits from a Composite Material of Silver Nanoparticles and Elastomeric Fibers. *Nat. Nanotechnol.* **2012**, *7*, 803−809.

(21) Sun, J. Y.; Zhao, X. H.; Illeperuma, W. R. K.; Chaudhuri, O.; Oh, K. H.; Mooney, D. J.; Vlassak, J. J.; Suo, Z. G. Highly Stretchable and Tough Hydrogels. *Nature* **2012**, *489*, 133−136.

(22) Zhao, S. F.; Zhang, G. P.; Gao, Y. J.; Deng, L. B.; Li, J. H.; Sun, R.; Wong, C. P. Covalently Bonded Nitrogen-Doped Carbon-Nanotube-Supported Ag Hybrid Aerogels: Synthesis, Structure Manipulation and Its Application for Flexible Conductors and Strain-Gauge Sensors. Revised.

(23) Ku-Herrera, J. J.; Aviles, F. Cyclic Tension and Compression Piezoresistivity of Carbon Nanotube/Vinyl Ester Composites in the Elastic and Plastic Regimes. *Carbon* **2012**, *50*, 2592−2598.

(24) Deville, S.; Saiz, E.; Nalla, R. K.; Tomsia, A. P. Freezing as a Path to Build Complex Composites. *Science* **2006**, *311*, 515−518.

(25) Wang, M.; Anoshkin, I. V.; Nasibulin, A. G.; Korhonen, J. T.; Seitsonen, J.; Pere, J.; Kauppinen, E. I.; Ras, R. H. A.; Ikkala, O. Modifying Native Nanocellulose Aerogels with Carbon Nanotubes for Mechanoresponsive Conductivity and Pressure Sensing. *Adv. Mater.* **2013**, *25*, 2428−2432.

(26) Kim, K. H.; Oh, Y.; Islam, M. F. Graphene Coating Makes Carbon Nanotube Aerogels Superelastic and Resistant to Fatigue. *Nat. Nanotechnol.* **2012**, *7*, 562−566.

(27) Zhao, S. F.; Qiu, S. C.; Zheng, Y. Y.; Cheng, L.; Guo, Y. Synthesis and Characterization of Kaolin with Polystyrene via In-situ Polymerization and Their Application on Polypropylene. *Mater. Des.* **2011**, *32*, 957−963.

(28) Boland, C. S.; Khan, U.; Backes, C.; ONeill, A.; McCauley, J.; Duane, S.; Shanker, R.; Liu, Y.; Jurewicz, I.; Dalton, A. B.; Coleman, J.

N. Sensitive, High-Strain, High-Rate Bodily Motion Sensors Based on Graphene−Rubber Composites. *ACS Nano* **2014**, *8*, 8819−8830.

(29) Tang, Y.; Gong, S.; Chen, Y.; Yap, L. W.; Cheng, W. L. Manufacturable Conducting Rubber Ambers and Stretchable Conductors from Copper Nanowire Aerogel Monoliths. *ACS Nano* **2014**, *8*, 5707−5714.

(30) Chelidze, T.; Gueguen, Y. Pressure-Induced Percolation Transitions in Composites. *J. Phys. D: Appl. Phys.* **1998**, *31*, 2877−2885.

(31) Luo, S.; Liu, T. SWCNT/Graphite Nanoplatelet Hybrid Thin Films for Self-Temperature-Compensated, Highly Sensitive, and Extensible Piezoresistive Sensors. *Adv. Mater.* **2013**, *25*, 5650−5657.

(32) Yao, H. B.; Huang, G.; Cui, C. H.; Wang, X. H.; Yu, S. H. Macroscale Elastomeric Conductors Generated from Hydrothermally Synthesized Metal-Polymer Hybrid Nanocable Sponges. *Adv. Mater.* **2011**, *23*, 3643−3647.

(33) Zou, J. H.; Liu, J. H.; Karakoti, A. S.; Kumar, A.; Joung, D.; Li, Q.; Khondaker, S. I.; Seal, S.; Zhai, L. Ultralight Multiwalled Carbon Nanotube Aerogel. *ACS Nano* **2010**, *4*, 7293−7302.

(34) Cao, A. Y; Dickrell, P. L.; Sawyer, W. G.; Ghasemi-Nejhad, M. N.; Ajayan, P. M. Super-Compressible Foamlike Carbon Nanotube Films. *Science* **2005**, *310*, 1307−1310.